Modelling flint acoustics for detection of submerged Stone Age sites

Jean-Pierre Hermand*, Ole Grøn†, Mark Asch*§ and Qunyan Ren*
*Environmental Hydroacoustics lab, Université libre de Bruxelles (U.L.B.)
av. F. D. Roosevelt 50, CP 194/05, B-1050 Brussels, Belgium
†Center for Maritime Archaeology, University of Southern Denmark
Niels Bohrs vej 9, DK - 6700 Esbjerg, Denmark
§ LAMFA CNRS-UMR6140, Amiens France.

***Abstract*—In accordance with the increasing industrial interests in the sea areas a two-pronged development can be observed: an appearance of new methodologies for up-to-date and cost-effective management and protection of these cultural areas and environmental resources which is underpinned by a parallel development of a legislative framework. For submerged cultural heritage UNESCO's Convention on the Protection of the Underwater Cultural Heritage (UNESCO 2001) forms an important part of this administrative development. The method for acoustic detection of submerged Stone Age sites outlined in this paper will, if it can be demonstrated to work in practice, contribute to the spectrum of ongoing new technologies facilitating access to large amounts of environmental data, useful for the understanding of environmental changes such as rising sea levels and their impact on human cultural systems in prehistory. This paper mainly addresses the acoustical characterization of buried flints for Stone Age underwater archaeology. A finite element time domain method is used to simulate acoustic remote sensing in a realistic environment. The method is capable of accurately representing the complex interplay between the acoustic waves, the sediments and the flints embedded in the cultural layer. The predicted signals, once compared with in-situ measurements, provide the basis for the solution of inverse problems that can pinpoint the presence of worked flint over large areas.**

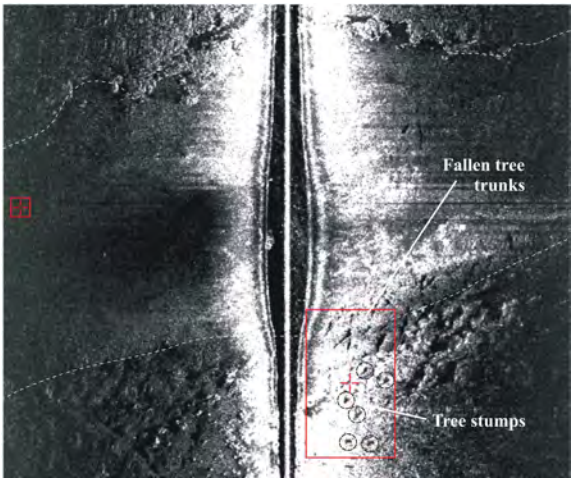

Figure 1: Side scan of a palaeo-channel close to the Møllegabet site with tree stumps and fallen tree trunks from about 5000 B.C. (7000 years old).

I. Introduction

Settlement archaeology under water normally creates associations to the investigation of submerged antique city areas with exposed physical structures such as Dwarka, India, Yonaguni-Jina, Japan & Piraeus, Greece etc. However, the resource-rich sea shores that more than 90–95% of the last 140,000 years have been considerably below what they are today hold a large number of very old Stone Age sites, of which some must be expected to have a degree of preservation (organic materials such as wood, plant fibres, bark etc.) that outnumbers what we know from dry land as shown in Fig. 2.

A lot of these sites will be destroyed by the wave activity of the falling and rising sea level, but experience shows that there normally also will be preserved smaller or larger pockets with sites and remains of prehistoric cultural landscapes, that can provide very important preserved environmental details elucidating the relation between human culture and the changing environment. From the Baltic we know - in relation to the Mesolithic Stone Age sites - extensive areas with drowned Stone Age forests - tree stumps which have in some cases the fallen trunks lying beside them (Fig. 1). There are submerged peat basins - former lakes - with Stone Age sites along their shores, and in a few cases very well preserved details of the earlier dry-land settlement surfaces have been investigated [1]–[5].

Where the 'direct' environmental information that can be extracted from preserved vegetation surfaces will be of high importance for future reconstructions of prehistoric climates and environments, the 'waste' DNA of fauna and flora that has been collected by the humans and absorbed by the submerged settlements' sediment seems to have a good chance of local survival under relatively cold and saline submerged conditions [6]–[8]. Thus an acoustic technology leading to a reliable mapping of the important submerged Stone Age sites at the same time will pinpoint the reservoirs of important ancient DNA for environmental studies.

As a central part of the development of an up-to-date management system for this important part of the submerged cultural heritage, there are now attempts to find technological approaches that facilitate an efficient and cost-effective localization of the submerged and sediment embedded Stone Age sites (Fig. 2(a)). An excavated example of the stratigraphy of a submerged Stone Age site is the registered section through the Stone Age dwelling pit at the site Møllegabet II (Fig. 2(b)).

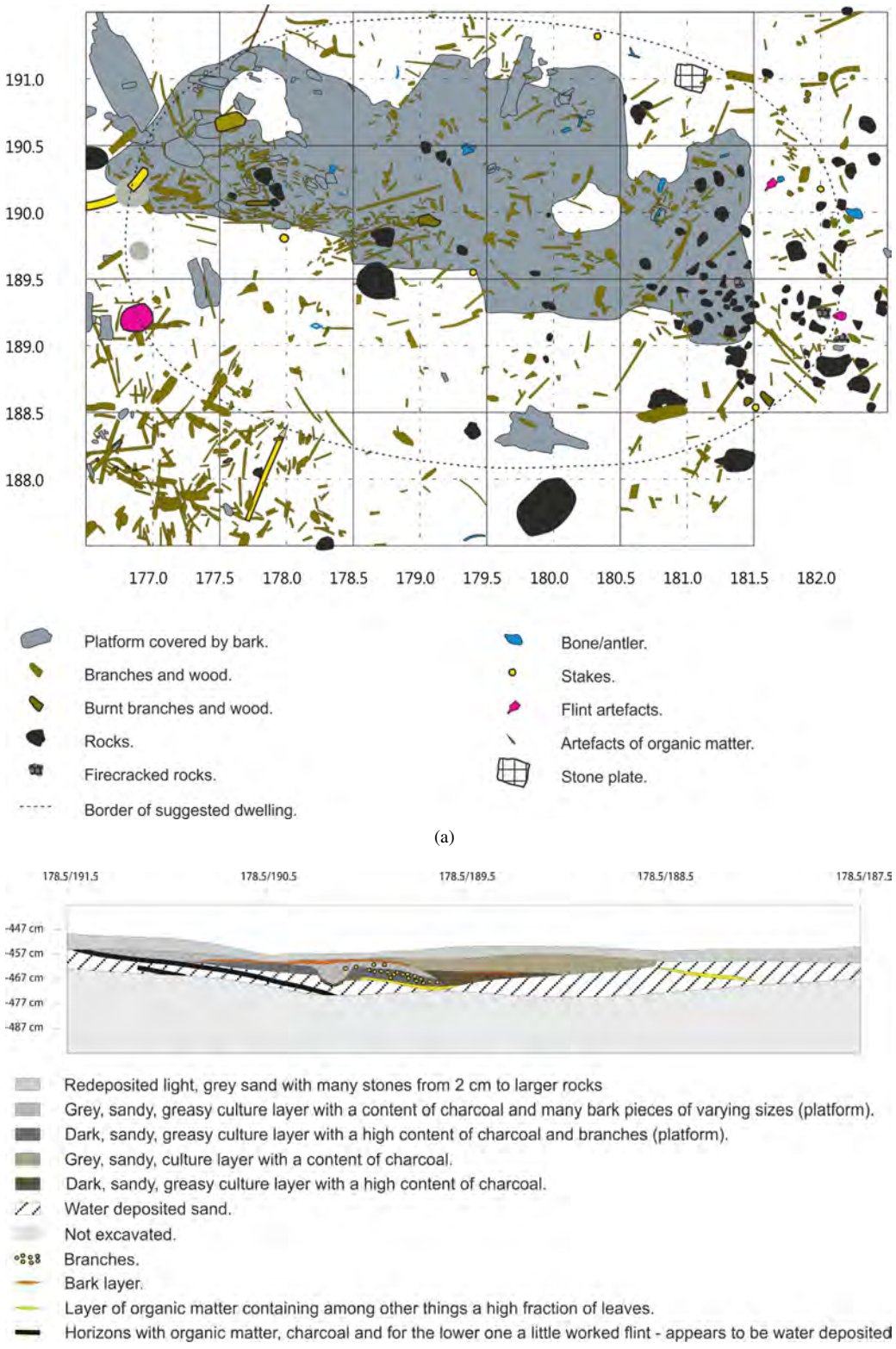

(a)

(b)

Figure 2: (a) Plan of the excavated Stone Age dwelling from Møllegabet II (dated to ca. 5000 BC). (b) Section through the dwelling pit above. All sandy layers contain a more or less significant fraction of organic material.

The dwelling was found just below the redeposited light gray sand, with a part of its features and finds embedded in this layer. All the sand layers described in Fig. 2(b) have a more or less significant content of organic matter, some of them so high that they could be characterized as sandy gyttja. The site is located on an old beach just on the edge of an inlet, today filled with an up to 1.5-m thick layer of marine gyttja. The unexcavated cultural layer - waste from the settlement - continues into this layer. The dwelling pit contained thousands of flint blades and flakes. To the south-west of the dwelling pit the gyttja layer, which contained the burial of a young man in a dugout canoe, also contained large amounts of flint blades and flakes 0–5-cm deep in it. Also here was on the top a layer of redeposited sand with a content of organic matter. There are not many excavated sites with their land surfaces preserved [2]. Often the preserved remains are the layers deposited in the water outside the sites. It is likely that the acoustic technique discussed here can reveal more sites with the settlement surfaces preserved.

The controlled removal of blades and flakes of flint or in some cases other silicate minerals from a larger body - a 'core' (flint knapping), which is the definitoric basis for the term 'Stone Age', involves an acoustic phenomenon that may be very useful for locating such sites. Stone Age sites often contain hundreds and often thousands of typical man-made blades and flakes whose typical acoustic parameters are given in Tab. II. For a better understanding of the acoustic phenomenon of flint knapping, sound lab experiments on sixteen flint blades and flakes from nine different Danish Stone Age sites were carried out by Rasmussen to analyse their: (a) energy at the different frequencies and (b) time delay of the different frequency components. The resonance peaks of all the analysed samples are shown in Fig. 3(b). At two sites the measurements were made on two different pieces of flint. The remaining measurements were made on only one flint blade or flake - an example shown in Fig. 4. The resonance signals were so strong, that the individual pieces had to be damped during the measurement, which did not change the spectral shape of the resonance signal. According to Rasmussen's suggestion, an accumulation of worked flint pieces will create a detectable signature in a narrow frequency band either as an amplification of a part of an incident acoustic wave or as absorption of a part of it. It is expected that damping by sediment would weaken the signal from the single buried flint pieces but not change their resonance spectral shape. Hence, it is believed that the resonance is a stable and detectable phenomena for flint pieces. The accumulation of resonances from worked flint pieces should thus create a detectable acoustical signature for underwater Stone Age archaeology.

In, e.g., [11]–[15], the target resonance feature has been demonstrated to be an effective tool for underwater buried target detection. Specific processing methods are also developed based on the resonance features for buried target detection on land, e.g., acoustic resonance spectroscopy (ARS) [16] and isolation and identification methodology for resonance (MIIR) [11]. Because these targets are often larger and with

(a)

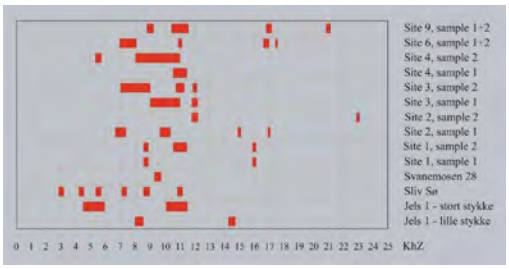

(b)

Figure 3: (a) Flint 'core' with thin and long 'blades' removed from it nearly like one peels a potato hitting the edge of the 'platform' which is in one end of the 'core'. (b) The peaks of all the flint blades and flakes resonance spectra measured by Rasmussen.

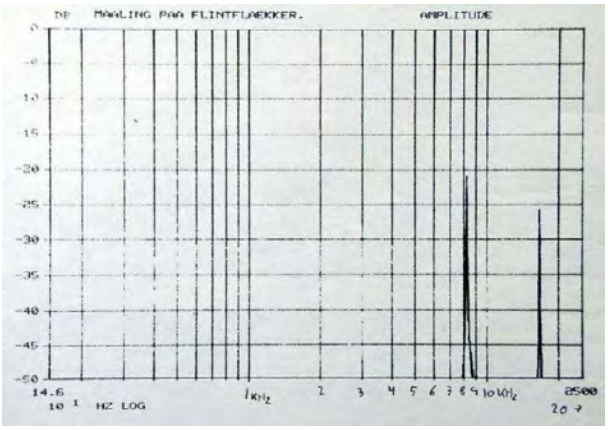

Figure 4: Resonance spectrum of one of the flint pieces measured by Rasmussen.

resonance characteristics different from those of flint blades and flakes, this method can not be applied directly to flint detection. In a former paper [9], the feasibility of using flint resonance for detection of underwater Stone Age sites was considered. A simple acoustic model [15] was employed that treats the flint resonance as single frequency component signals that can be excited by a broadband sound source under certain conditions. Thus the flint detection problem becomes equivalent to the detection of resonances from bottom reverberation noise. Wavelet transform (WT) [10] and

frequency domain WT (FDWT) [13] were used to extract specific resonance features from the scattered signals and thus to discriminate the flint pieces from other scattering objects. In that paper, the WT decomposition coefficients display a slightly different structure than those of resonance signal and reverberation, especially for the fourth level coefficients. Since the resonance features are better resolved in the frequency domain, larger differences were obtained using FDWT. Such differences between reverberation and resonance signals can possibly be used in, e.g., support vector machines (SVM) [18], for the flint pieces discrimination.

Nevertheless the resonance model used in [9] is an approximation that may not hold in a real situation. The resonances of a flint piece are likely difficult to excite when embedded in a sediment layer with complex boundary conditions. Therefore commonly used ARS and MIIR methods and the method proposed in [9] may turn out to be ineffective. A better understanding of the interaction between the flint piece and a probing acoustic signal will certainly enhance its detection. In this paper, a realistic environment is considered: a near-coastal, shallow-water section (parallelepiped-shaped) with a water layer overlying one or more sediment layers, within which, flint blades or flakes are embedded in a so-called cultural layer. An acoustic source signal is used to probe that layer with the aim of detecting the presence of worked flints. The signals received on an array of hydrophones are predicted and in the future will be compared to actual measurements *in situ*. Hence the inverse problem of detecting and locating the flints from far-field measurements can be solved with the aid of numerical modelling and simulation.

Traditionally, finite-difference methods have been widely used for numerical simulations of acoustic (and seismic) wave propagation in an underwater context with both fluid and solid layers [19]. In this paper, a finite-element time-domain (FETD) method is used to simulate the acoustic signals scattered from flint and no-flint regions, with the aim of finding differences that are usable for *in-situ* flint detection.

The rest of the paper is organized as follows. Section II describes the environment of submerged Stone Age cultural landscapes. Section III explains the acoustic propagation model used in this paper. Numerical simulation results are then presented in Sec. IV for individually-spaced flints and flint clusters. Section V concludes the paper.

II. Submerged Stone Age environment model

The Danish Baltic has since the 60s served as an experimental area for development of new methods for excavation and management of submerged Stone Age sites. Møllegabet I was the first site where systematic excavation started in 1976. Shortly after excavation of Tybrind Vig started [4]. A series of highly informative excavations have followed since then, and a basic administrative procedure for management and protection of these sites has been developed.

It is important to understand that the submerged Stone Age cultural landscapes in large areas will have been erased by the wave dynamics of the rising and falling sea level and the currents, that for instance in the central parts of the Danish belts leave little more than the worn moraine bottom with truncated remains of prehistoric peat basins. However, experience shows that there normally exist pockets where cultural landscapes with standing Stone Age tree trunks and sometimes the fallen tree trunks lying beside them on the old forest floor are preserved (Fig. 1). Along the banks of the old shore lines and lakes/peat basins Stone Age sites can be preserved with all their organic materials preserved, such as bark, twigs, nuts, fruit stones, bones of their prey animals, dwelling remains etc.

Such sites have served as centres for extraction of the environmental resources exploited by the human hunter-gatherers. Large amounts of meat from prey animals, fish, birds, seeds, nuts, roots etc, have been concentrated here and thus wasted material from the collected species (blod, urine, juice, etc.) should provide a good chance of DNA preservation in the relatively cold and saline submerged sediments [6]–[8]. Therefore the well preserved submerged Stone Age settlements must be regarded as important cultural as well as environmental heritage.

Well preserved submerged settlement remains will often be related to areas with soft sediments (e.g., Fig. 2(b)), such as peat and gyttja that according to the authors' experience permit good acoustic penetration with high-resolution equipment at frequencies between 1 kHz and 20 kHz. Often there will be a somewhat dynamic 'sand layer' covering the sea floor. This however will normally contain a significant organic component that also provides good penetration. Marine sediments such as sand/gravel with no organic content which - depending on their thickness - can be difficult to penetrate and clay will normally be located below the layers related to human activity at least where these belong to the Holocene and Late Glacial phases. Thus the acoustic 'access' to such well-preserved submerged Stone Age sites as well as a number of earlier sites must be expected to be quite promising. According to Fig. 2(b), a multi-layer sediment model is built for the following numerical simulations, whose sediment layer properties are given in Tab. I. An illustration of the environment model with flint clusters in shown in Fig. 6.

III. Finite-element time-domain modelling of acoustic propagation

To model acoustic wave propagation in a layered fluid-solid environment, the propagation of compressional waves in the fluid domain and compressional plus shear waves in the solid domain with appropriate initial and boundary conditions need be solved.

For the ocean-acoustic model used here, the elastic (acoustic-seismic) wave equation is adapted to each domain (and the layers within the solid domain) through the specification of the appropriate Lamé coefficients. This equation can faithfully model the water layer and has the further advantage of being able to reproduce the interplay of transversal, longitudinal and interface (Scholte) waves in, and between, the elastic layers. In particular, the correct modelling of the flint

interaction with the surrounding sediments is possible. This equation can be written as

$$\rho \boldsymbol{u}_{tt} - (\lambda + 2\mu)\nabla\nabla \cdot \boldsymbol{u} - \mu\Delta\boldsymbol{u} = f, \tag{1}$$

where $\boldsymbol{u} = (u_1, u_2, u_3)$ is the displacement in the x-, y- and z-direction, λ and μ are the Lamé coefficients, ρ is the medium density and f is an initial impulse that represents the acoustic source. The relations between these coefficients and the wave speeds are

$$c_p^2 = \frac{\lambda + 2\mu}{\rho} \qquad \text{and} \qquad c_s^2 = \frac{\mu}{\rho},$$

where c_p is the pressure (or primary) wave speed and c_s is the shear (or secondary) wave speed. Thus an acoustic layer is obtained in the model by simply setting $\mu = 0$ locally.

It is noted that the elastodynamic system (1) can also be expressed in displacement-stress form, component-by-component, as

$$\begin{aligned} \rho\frac{\partial u_i}{\partial t^2} &= \frac{\partial \sigma_{ij}}{\partial x_j} + f_i\,, \\ \sigma_{ij} &= \lambda\delta_{ij}\epsilon_{kk} + 2\mu\epsilon_{ij}\,, \\ \epsilon_{ij} &= \frac{1}{2}\left(\frac{\partial u_i}{\partial x_j} + \frac{\partial u_j}{\partial x_i}\right), \end{aligned} \tag{2}$$

where Einstein's summation convention is used for the indices, and δ is the Kronecker delta function. The advantage of the system (1) or (2) is that it intrinsically models *all* the different types of waves that can arise in layered media - compressional and shear waves in the bulk, Love, Stoneley and Raleigh waves along the interfaces.

A. Boundary and initial conditions

At the surface water, a pressure-release boundary condition is specified. Between layers, continuity conditions on the normal components of u and the stresses must be satisfied. At the bottommost level, a suitable absorbing condition is given. On the lateral boundaries, suitable absorbing/radiating conditions are specified.

The initial condition is a Ricker wavelet with the desired frequency content, located at the source position in the water layer. The hydrophones are "simulated" by simply recording the solution at given points.

B. On solutions to the inverse problem

The final aim is to detect the presence of flints embedded in the cultural layer by acoustic remote sensing. If an individual piece or a cluster of flints are considered as a source of diffracted waves, the inverse problem can be formulated as a source-detection type. An alternative formulation would be to detect the rapid changes in the compressional and shear speed profiles due to the outstanding characteristics of the flint material. Another option is to detect the flint pieces by identifying their typical resonances (between 4 kHz and 20 kHz) as measured in laboratory conditions through analysis of the frequency content of the returned signals.

The first two inverse problems can be formulated and solved by using an adjoint approach. Such an approach has been successfully employed in a number of underwater acoustic problems [24]–[26]. Briefly, the adjoint approach provides an analytical or a numerical gradient of a mismatch cost function, that is then employed for a rapid, gradient-based minimization of the cost function. This leads to an "optimal control" that solves the inverse problem: flint detection and localization.

C. Finite-element model

The most commonly used finite element formulations are classical Galerkin and spectral Galerkin, and the latter is chosen here for its greater accuracy and ability to deal effectively with smaller spatial scales. Because of the high degree polynomial spatial approximation and a hexahedral mesh, the spectral element method (SEM) provides an extremely efficient numerical model for acoustic-seismic wave propagation. In fact, the hexahedral elements produce a diagonal mass matrix and thus vastly improve the simulation CPU-times needed for time-domain simulations. Simulations are based on the SPECFEM code of Komatitsch et al [23] that can be adapted to treat the variable sound speed profile present in the shallow water layer. In addition, CAD software has been used to include accurate, 3D geometrical representation of the worked flint pieces.

The mesh construction is important for precise simulation of wave propagation. It must respect all the geometrical discontinuities and provide the possibility of mesh refinement and coarsening that maintain a constant number of elements per wavelength, everywhere in the model, as the wave speeds vary with depth. This yields a consistent numerical resolution throughout the modelled region.

IV. Numerical results

In this section, preliminary results obtained with the 2D version of SPECFEM and simplified models of single flint piece and flint cluster are shown.

A. Physical problem parameters

The acoustic geometry and environmental model (Figs. 5 and 6) used in the numerical simulations consists of:

- a seawater layer of 2-m depth with a source at 0.5-m height above the seafloor and and an horizontal array of hydrophones spaced by 0.1 m at the same depth;
- sediment layers of constant thickness: 10-cm sand, 20-cm mud, 5-cm cultural layer and 15-cm sand;
- flint blades and flakes randomly distributed in the cultural layer with orientation close to the horizontal, acoustic properties of typical flint material are given in Tab. II.

B. Individually spaced flints

1) Arbitrary source frequency: The first simulation test attempts to show the effect of flint presence in acoustic pressure signals. A source emits a Ricker pulse at the source position, $x_s = 1.5$ m, $z_s = -1.5$ m (circle in Fig. 6), with a central frequency at 4.5 kHz. Ten hydrophones, $H_1, \ldots, H_{10}$,

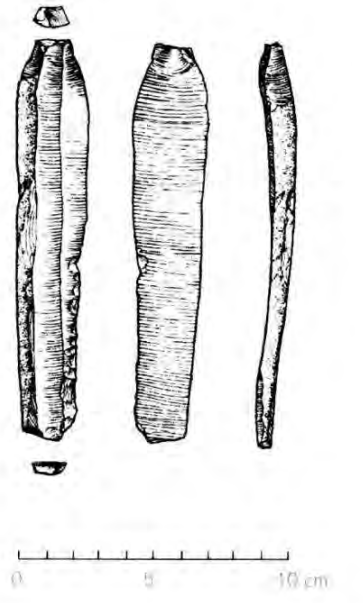

Figure 5: Flint and flake geometries.

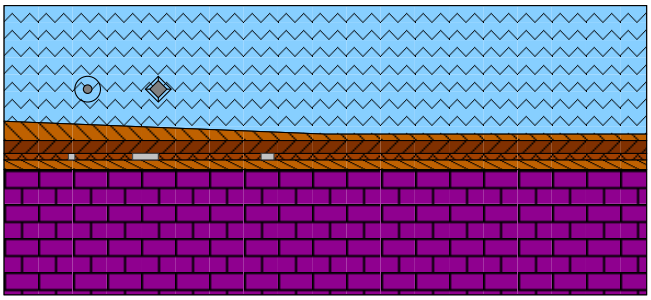

Figure 6: 2D, range-dependent environment with six layers whose properties are given in Tab. I. The source (circle) and the rightmost hydrophone (lozenge) of an horizontal line receiver array with 10 elements, 10-cm spaced, are shown. The grey boxes represent three flint clusters in the cultural layer. Overall dimensions are 10 m in range by 5 m in depth. The origin of (x, z) is at the left top of the box.

Table II: Acoustic parameters of typical flint material [20], [21].

Density	2300 kg/m^3
Compression speed	8433 m/s
Shear speed	5843 kg/m^3
Young's module	185 GPa
Poisson's Ratio	0.27

Table III: Predicted fundamental resonance frequencies of flint pieces of different lengths using Eq. 3.

Length (cm)	Resonance frequency (kHz)
8	17.72
10	14.18
12	11.82
14	10.13

are placed at depth $z = -1.5$ m, and at positions from $x = 1.6$ m to $x = 2.6$ m with 10-cm intervals. In Fig. 6, the lozenge indicates the position of hydrophone H_{10}. Three flint pieces of different sizes are placed in the cultural layer, whose dimensions correspond to those in Fig. 5. The three flints have lengths of $l_1 = 10$ cm, $l_2 = 12$ cm and $l_3 = 8$ cm and are centered at positions $x_1 = 1.55$ m, $x_2 = 1.8$ m and $x_3 = 2.1$ m. They are thus located at half range between the source and hydrophones H_1, H_5 and H_{10}, respectively. Their thickness is taken as 5 mm and they are placed at slightly different depths in the cultural layer. It is emphasized that these flint pieces are not represented in Fig. 6 which deals with the flint clusters discussed later. The FETD simulations use a 9-th order spectral approximation, 44 800 quad elements (90 400 points), 50 000 time steps with $dt = 6.25 \times 10^{-8}$ s and run in parallel, using MPI, in just over 55 minutes on an 8-core workstation.

Figure 7 compares received array signals with flints and with no flint. The three hydrophones placed symmetrically with respect to the flint pieces are shown. The first arrivals at times 0.07 ms for H_1, 0.4 ms for H_5 and 0.7 ms for H_{10} correspond to the direct paths between the source and the respective receivers. These are followed by weak bottom-reflected arrivals and stronger surface-reflected arrivals with a phase reversal. The bottom returns show a noticeable difference between the flints and no-flint situations in term of

Table I: Bottom layer properties. The cultural layer contains the flint blades and flakes (whose properties are given in Tab. II). The layer thicknesses in parentheses are the ones used in the presented acoustic simulations.

Layer	Thickness (cm)	ρ (kg/m^3)	c_p(m/s)	c_s(m/s)	α_p(dB/λ)	α_s(dB/λ)
seawater	0 – 500 (200)	1000	1500	–	–	–
sand	10 – 25 (10)	1900	1650	110	0.8	–
mud	20 – 30 (20)	1500	1500	50	0.2	–
cultural	5 – 10 (5)	1500	1500	50	0.2	–
sand	15 – 50 (15)	1900	1650	110	0.8	–
substrate (moraine)	semi–∞	2100	1950	600	0.4	1.0

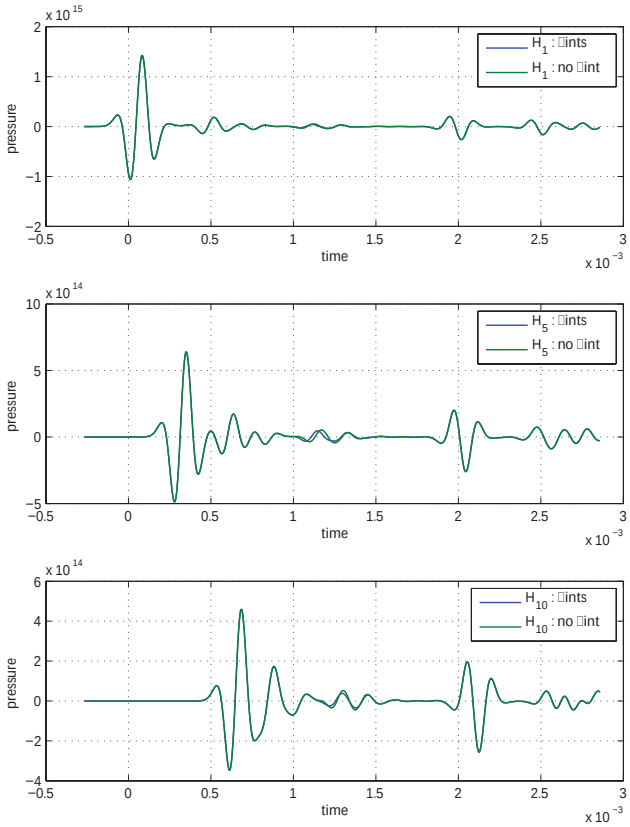

Figure 7: Comparison of the flints and no-flint signals received on hydrophones 1, 5 and 10 for a source frequency of 4.5 kHz.

their amplitude and arrival time. The differences between the three receivers relate to the changing angle of incidence and size of the respective flint pieces. This is better seen in Fig. 8 that shows the difference between the flints and no-flint signal envelopes for each hydrophone. There is a shorter delay and a smaller amplitude when a flint is present at the mid horizontal distance between the source and a receiver. These simulation results suggest that presence of an individual flint piece can possibly be detected by analyzing the signal in a time interval to the cultural layer depth (starting here at about 0.8 ms for the present source-receiver geometry and layers thicknesses).

2) Source frequency near flint resonance: To predict the resonance frequency of a flint piece [9], the extensional vibration model [22] was adopted. This model approximates a flint blade or flake (Fig. 3(a)) as a thin plate with thickness h, width w and length l. For a flint piece that satisfies $l \gg w \gg h$, its extensional vibration is equivalent to the vibration when split from a core by knapping. The resonance frequency for such vibration can be written as [22]:

$$f = \frac{m}{2l}\sqrt{\frac{E}{\rho}}\,, \tag{3}$$

where E and ρ are the Young's modulus and density of the flint material, respectively, and $m = 1, 2, 3$, etc.

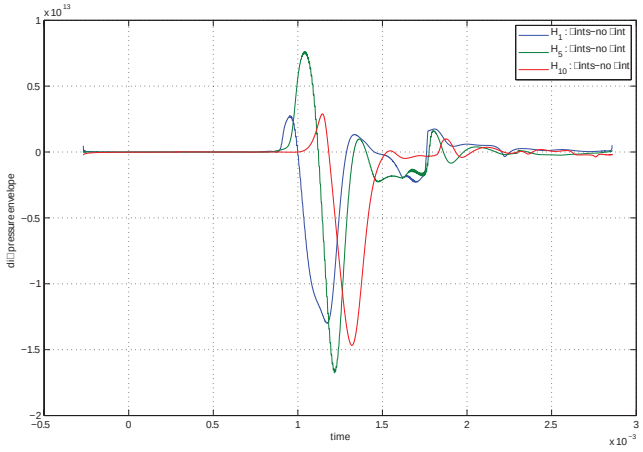

Figure 8: Differences of the flints and no-flint envelopes of the signals shown in Fig. 7.

The calculated fundamental resonance frequencies ($m = 1$) for different flint lengths are given in Tab. III. Though the predicted frequencies are consistent with the resonance frequency band measured by Rasmussen it is noted that the resonance frequency for the extensional vibration will gradually decrease as the width of the flint piece is increased [22]. Experimental data of the resonance frequency of a thin plate are given in Fig. 7.6 of Ref [22]. Accordingly, the actual resonance frequency of a flint piece with a thickness of 5 mm will be lower than the predicted values given in Tab. III.

The second simulation aims to test whether one can obtain more information from the received signals using a source signal with the approximate resonance frequency of a given flint. For limiting the computational time the source-receiver geometry is different and the domain smaller than in the previous test. The source frequency is set to 14 kHz which corresponds to the resonance frequency of a very thin flint piece of 10-cm length (Tab. III). As for the first test the thickness is set to 5 mm yielding an actual resonance frequency expected to be a bit lower than 14 kHz.

Figure 9 shows the resulting pressure signal received on hydrophone 10. Similar to the former simulation, a difference appears when the signal interacts with the sediment embedded flint. However, here the difference is not only in the wave amplitude but also in the waveform. The flint resonance frequency may be excited by the source signal and its value may be slightly different than the central frequency of the source which results in the waveform difference. The larger difference may provide more information for flint detection.

C. Flint clusters

A third simulation test deals with a more realistic environment. Three flint clusters are modeled by a simplified, rectangular geometry and placed in the cultural layer. The three clusters have horizontal extensions of $l_1 = 10$ cm, $l_2 = 53$ cm and $l_3 = 21$ cm and are centered at positions $x_1 = 1.1$ m, $x_2 = 2.4$ m and $x_3 = 4.3$ m. Their thickness is

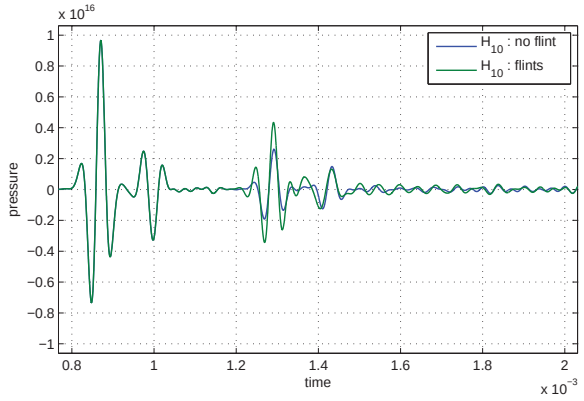

Figure 9: Comparison of the signals received on hydrophone 10 in the presence and absence of the flint pieces. The source frequency of 14 kHz is close to the fundamental resonance of the 10-cm flint.

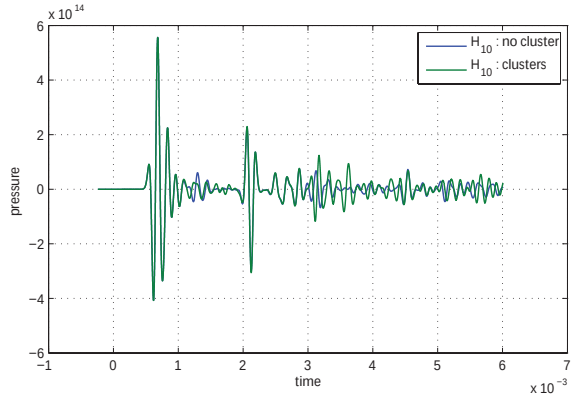

Figure 10: Comparison of the signals received on hydrophone 10 in the presence and absence of the flint clusters, for a source frequency of 5 kHz.

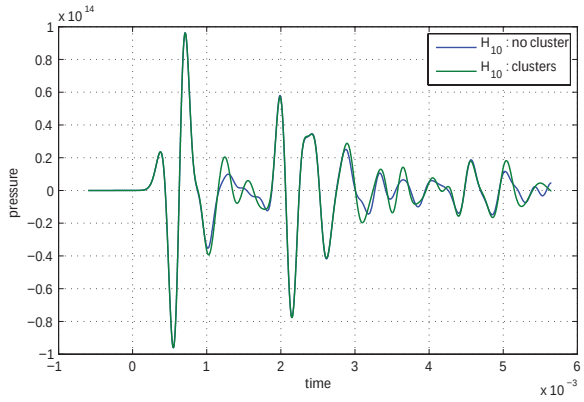

Figure 11: Comparison of the signals received on hydrophone 10 in the presence and absence of the flint clusters, for a source frequency of 2 kHz.

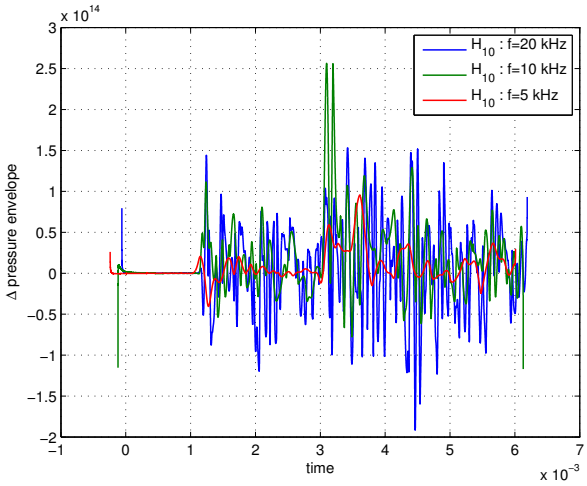

Figure 12: Difference of the received signal envelopes in the presence and absence of the flint clusters. Results are shown for hydrophone 10 and the source frequencies of 5, 10 and 20 kHz.

that of the cultural layer, i.e., 5 cm. A source emits a Ricker pulse at the source position, $x_s = 1.5$ m, $z_s = -1.5$ m, with central frequencies of 1 kHz, 2 kHz, 5 kHz, 10 kHz and 20 kHz. Ten hydrophones, $H_1, \ldots, H_{10}$, are placed at depths $z = -1.5$ m, and at positions from $x = 1.6$ m to $x = 2.5$ m with 10-cm intervals.

The simulations use a 9-th order spectral approximation, 10 152 quad elements (20 605 points), 50 000 time steps with $dt = 1.25 \times 10^{-7}$ s and run in parallel, using MPI, in just over 7 minutes on an 8-core workstation.

The effects due to the presence of the flint clusters can be clearly observed in the pressure signals, as recorded by the hydrophones. Figures 10 and 11 show the results for source frequencies of 2 kHz and 5 kHz, respectively. For both frequencies there are clear differences in the signals obtained with and without the flint clusters. In these two plots, the portion of signal between about 0.4 ms and 1 ms comprises the direct and sediment-surface reflected signals. The first interval where differences are observed between about 1 ms and 1.7 ms is related to sediment-refracted and flint-cluster-reflected signals. The nearly identical signals between 1.7 ms and 2.6 ms being water surface-reflected signals are obviously unaffected by the flint cluster presence. These are followed by the water surface-reflected, sediment-refracted and flint-cluster reflected signals which again exhibit differences. The signals recorded on the other hydrophones give similar results.

Figure 12, shows the pressure envelope differences ("flint cluster" minus "no flint cluster") of the pressure signal measured on hydrophone 10 for source frequencies of 2, 5 and 20 kHz. The result of 10-kHz signal shows the most pronounced difference for the flint cluster at mid horizontal distance between the source and hydrophone 10.

V. Conclusion and perspective

A submerged Stone Age site was modelled as a fully range-dependent, bottom-layered, shallow-water environment. A time-domain spectral finite element method computed received array signals due to a probing acoustic signal. 2D acoustic simulations show that the presence of individually-spaced flints or clusters embedded in the cultural layer is clearly detectable. These promising numerical results are a first step toward solving the 3D inverse problem of flint detection and localization.

Acknowledgment

Development of an acoustic system for the location of Stone Age cultural layers is one of the projects related to the SPLASHCOS network project funded by the COST Programme of the EU. 3D scanning of flint blades and flakes and creation of 3D models was kindly provided by Søren Kvejborg, the company Kvejborg, DK.

References

[1] O. Grøn, "The investigation of submerged Stone Age landscapes using diving as a research tool: an example from Denmark". *International Journal of the Society for Underwater Technology*, Vol.27, No.3. pp.109–114, 2007.

[2] J. Skaarup and O. Grøn, "Møllegabet II. A submerged Mesolithic settlement in southern Denmark", *BAR International Series 1328*, Oxford, 2004.

[3] H. Lübke, U. Schmölcke, and F. Tauber, "Mesolithic hunter-fishers in a changing world: a case study of submerged sites on the Jackelberg, Wismar Bay, northeastern Germany". edited by: Benjamin, J., Bonsall, C., Pickard, C., Fischer, A. *Submerged Prehistory, Oxbow Books*, Oxford. pp.21–37, 2011.

[4] O. Grøn and J. Skaarup, "Submerged Stone Age coastal zones in Denmark: investigation strategies and results. Submarine prehistoric archaeology of the North Sea. Research priorities and collaboration with industry", *CBA Research Report 141*, edited by N.C. Flemming, pp.53–56, 2004.

[5] O. Grøn, A. Nørgåard Jørgensen, and G. Hoffmann, "Marine archaeological survey by high-resolution sub-bottom profilers", *Norsk Sjøfartsmuseums Årbok 2004*, pp. 115–144.

[6] M. Hansson, and B. Foley, "Ancient DNA fragments inside classical Greek amphoras reveal cargo of 2400-year-old shipwreck". *Journal of Archaeological Science* Vol.35., No.5 pp.1169-1176, 2008.

[7] E. Willerslev, A. J. Hansen, J. Binladen, T. B. Brand, M.T.P. Gilbert, B. Shapiro, M. Bunce, C. Wiuf, D. A. Gilichinsky, and A. Cooper, "Diverse plant and animal genetic records from holocene and pleistocene sediments". *Science* Vol. 300, No.2. pp.781–795, 2003.

[8] E. Willerslev, A. J. Hansen, and H. N. Poinar "Isolation of nucleic acids and cultures from fossil ice and permafrost". *TRENDS in Ecology and Evolution*" Vol.19 No.3, pp.141–147, 2004:.

[9] Q. Y. Ren, O. Grøn and J.-P. Hermand. On the in-situ detection of flint for Stone Age underwater archaeology. in *Oceans'11 Santander*, Spain, 2011.

[10] I. Daubechies, "The wavelet transform, time-frequency localization and signal analysis", *IEEE Transactions on Information Theory*, vol.36(5), pp.961–1005, 1990.

[11] D. Décultot, K. Cacheleux, and G. Maze,"Detection and classification of an object buried in sand by an acoustic resonance spectrum method," in *International Conferences on Detection and Classification of Underwater Targets*, Edinburg, UK 2007, Proceeding CD Vol. 29, Pt. 6, 2007.

[12] X. K. Li, "Study on characteristic extraction and identification of mine targets", Doctor thesis (in Chinese), Harbin Engineering University, Harbin, 2000.

[13] X. K. Li, T. T. Li, and Z. Xia, "Feature extraction and fusion based on the characteristics of underwater targets", *Journal of Harbin Engineering University* (in Chinese), vol. 31(7), pp. 903–909, 2010.

[14] D. Décultot, R. Liétard, and G. Maze, "Classification of a cylindrical target buried in a thin sand-water mixture using acoustic spectra," *The Journal of the Acoustical Society of America*, vol. 127, pp. 1328–1334, 2010.

[15] R. Wang, H. Y. Wang, Y. F. Zhang, and Z. Zhu, "One research of method on the anti-reverberation to promote the performance of echo detection", in *Proceeding of the China middle and eastern acoustic meeting* (in Chinese), 2008.

[16] D. N. Sinha, "Acoustic resonance spectroscopy," *IEEE Potentials*, vol. 11(2), pp. 10, 1992.

[17] http://en.wikipedia.org/wiki/Acoustic-resonance

[18] B. Schölkopf, C. Burges and A. Smola, "Making large-scale SVM learning practical. Advances in kernel methods-support vector learning," *MIT-press*, 1999.

[19] M. J. Buckingham, Ocean-acoustic propagation models. J. Acoustique, 223–287, 1992.

[20] http://www.ioffe.ru/SVA/NSM/Semicond/Si/mechanic.html.

[21] http://cofrest.info/md15.html.

[22] H. J. McSkimin, "Theoretical analysis of modes of vibration for isotropic rectangular plates having all surfaces free," *Bell Sys. Tech. Jour*, vol. 23 pp. 151–177, 1944.

[23] J. Tromp, D. Komatitsch, and Q. Liu. Spectral-element and adjoint methods in seismology. Communications in Computational Physics, 3(1): 1–32, 2008.

[24] J.-P. Hermand, M. Meyer, M. Asch, and M. Berrada, "Adjoint-based acoustic inversion for the physical characterization of a shallow water environment," *J. Acoust. Soc. Amer.*, vol. 119, pp. 3860–3871, June 2006.

[25] M. Meyer, J.-P. Hermand, M. Asch, and J.-C. Le Gac, "An iterative multiple frequency adjoint-based inversion algorithm for parabolic-type approximations in ocean acoustics," *Inverse Problems in Science and Engineering*, vol. 14, pp. 245–265, Apr. 2006.

[26] M. Meyer, J.-P. Hermand, M. Berrada, and M. Asch, "Remote sensing of Tyrrhenian shallow waters using the adjoint of a full-field acoustic propagation model," Journal of Marine Systems. Special issue on Coastal Processes: Challenges for Monitoring and Prediction, vol. 78, pp. S339–S348, Nov. 2009.